catalysts

MDPI

Review

Photoelectrochemical Conversion of Methane into Value-Added Products

Adeel Mehmood [1], Sang Youn Chae [2] and Eun Duck Park [1,3,*]

[1] Department of Energy Systems Research, Ajou University, Suwon 16499, Korea; adeelmkhank007@ajou.ac.kr
[2] Institute of NT-IT Fusion Technology, Ajou University, Suwon 16499, Korea; ekachemist@gmail.com
[3] Department of Chemical Engineering, Ajou University, Suwon 16499, Korea
* Correspondence: edpark@ajou.ac.kr

Abstract: Methane has been reported to be directly converted into value-added products through various methods. Among them, photoelectrochemical (PEC) methane conversion is considered an eco-friendly method because it utilizes solar light and is able to control the selectivity to different products by means of application of an external bias. Recently, some PEC methane conversion systems have been reported, but their performance efficiencies are relatively lower than those of other existing thermal, photocatalytic, and electrochemical systems. The detailed mechanism of methane activation is not clear at this stage. In this review, various catalytic materials and their roles in the reaction pathways are summarized and discussed. Furthermore, promising semiconductor materials, co-catalysts, and oxidants have also been proposed. Finally, direct and indirect pathways in the design of the PEC methane conversion system have been discussed.

Keywords: methane activation; photoelectrochemical conversion; oxidation; methanol; formic acid

Citation: Mehmood, A.; Chae, S.Y.; Park, E.D. Photoelectrochemical Conversion of Methane into Value-Added Products. *Catalysts* **2021**, *11*, 1387. https://doi.org/10.3390/catal11111387

Academic Editor: Nicolas Alonso-Vante

Received: 19 October 2021
Accepted: 14 November 2021
Published: 17 November 2021

1. Introduction

Methane is a major ingredient in biogas, natural gas, coal-bed gas, shale gas, and gas hydrates. In addition to conventional natural gas, unconventional natural gas, including shale gas, coal-bed gas, and tight gas, have also recently attracted much attention for methane extraction, because of their abundance [1,2]. Since methane has the highest H/C ratio and heat of combustion among hydrocarbons, it is utilized as a fuel for transportation and heating, and for industrial uses. The combustion of methane produces 20–25% of the total global carbon dioxide (CO_2) emissions [3]. Since methane is a worse greenhouse gas than CO_2, 3.5% of natural gas is flared during its production and is not released into the atmosphere [3]. Methane can be exploited with less impurities such as sulfur and metal than the oils and coal present in nature, thus making its utilization as a chemical feedstock highly desirable. However, the chemical activation of methane faces many obstacles because of its inert properties.

The CH_4 molecule is very stable and symmetrical, with low polarizability (2.84×10^{-40} $C^2 \cdot m^2 \cdot J^{-1}$) owing to the low electronegativity difference between hydrogen and carbon atoms [4]. Thus, a relatively strong local electric field is required to cause the polarization of CH_4 to initiate electrophilic or nucleophilic chemical reactions. In comparison to other alkanes, CH_4 has only four strong localized C–H bonds, with a bond energy of 439.3 $kJ \cdot mol^{-1}$ at standard temperature and pressure [5]. As a result, CH_4 cannot undergo homolytic or heterolytic C–H bond scissions. Methyl cations (CH_3^+) are unstable among carbocations, making methane the least reactive alkane in terms of hydride ion abstraction. It also shows low reactivity towards acids and bases due to its weak acidity ($pK_a \approx 48$) and low proton affinity (543.9 $kJ \cdot mol^{-1}$) [4]. Therefore, the chemical transformation of methane generally requires harsh reaction conditions.

Most commercial chemical processes from methane are based on an indirect pathway, which first involves the production of syngas ($CO + H_2$), followed by subsequent chemical

processes to synthesize various platform chemicals through C1 chemistry. Since the first syngas synthesis is a highly energy-intensive process, this indirect pathway can have its economical merits only with large-scale plants, which can be applied to only some natural gas wells with an extensive reservoir. To utilize small natural gas resources, there is a need for the direct transformation of methane into value-added chemicals.

The partial oxidation of methane has received intensive attention for the direct conversion of methane into platform chemicals, because potential products such as methanol, ethanol, and formic acid have economic advantages (Figure 1).

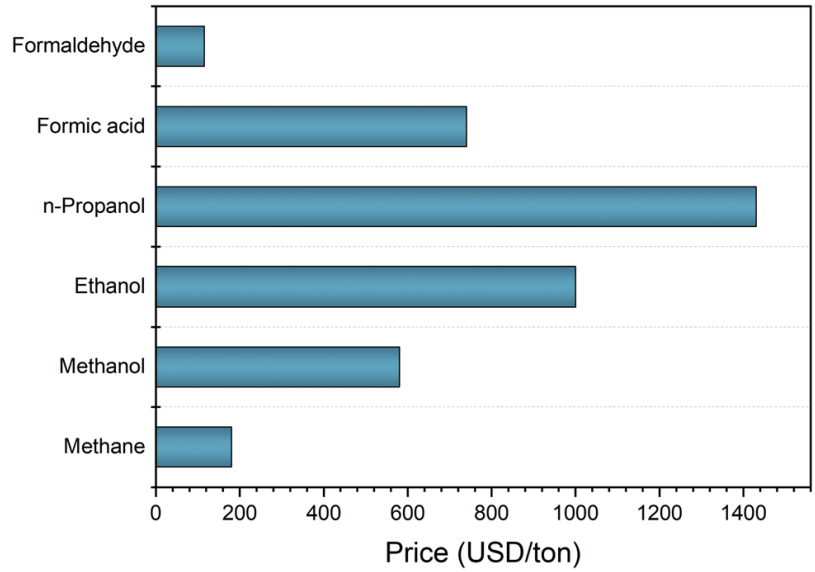

Figure 1. Price comparison of various oxygenated products produced from the methane oxidation reaction [6]. Copyright 2020, Royal Society of Chemistry.

The partial oxidation of methane at low temperatures is a kinetically sluggish process [7]. Typically, a substantial amount of energy is required to break the C–H bonds and oxidize the CH_4 molecule to produce oxygenated products (excluding CO_2). Usually, this energy is provided by increasing the temperature of the system. Practically, the oxidation of CH_4 should always be conducted at high temperatures (>700 °C), which often results in reactions being mediated by a free radical pathway with inherently low selectivity [4]. High-temperature conditions, which are often accompanied by high pressures, cause high costs and safety issues on a commercial scale. Moreover, the energy required to break down the C-H bond of methane is higher than that of partially oxidized chemicals, resulting in the production of the fully oxidized product (CO_2). For example, the dissociation energy of the C–H bond in CH_3OH is 0.4 eV less than that of CH_4. The low solubility of gaseous CH_4 in comparison to other highly soluble oxidized products from methane poses an additional challenge in liquid-phase methane oxidation [8]. To avoid side reactions, recent studies on selective methane conversion have been conducted under mild conditions. However, at low reaction temperatures, methane can be activated by providing external energy through light and/or electricity or by adding strong oxidants, including H_2O_2. Figure 2 summarizes the significance and challenges of CH_4 oxidation.

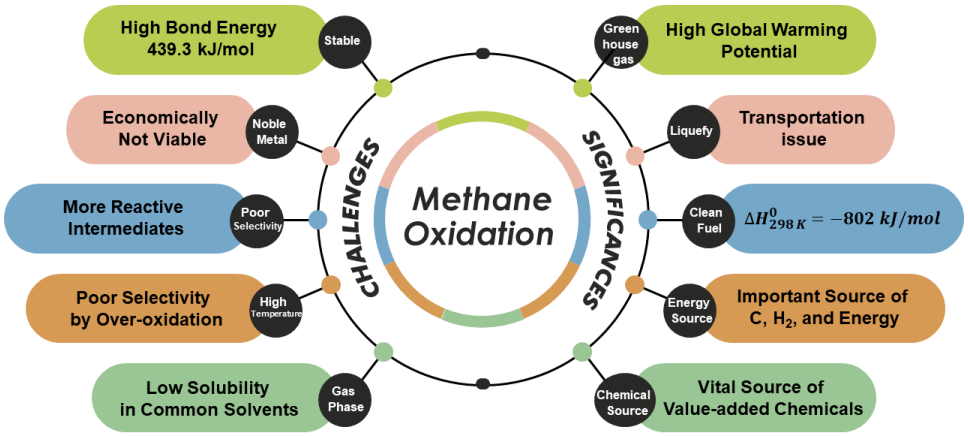

Figure 2. Challenges in and significance of CH_4 oxidation.

2. Photoelectrochemical (PEC) Methane Oxidation

Generally, the partial oxidation of methane into useful oxygenated products can be carried out by means of thermal reactions under high temperature and high-pressure conditions. Currently, direct methane oxidation to C_1 oxygenated products (methanol, formic acid, and formaldehyde) has been extensively studied in both liquid and gas phases under mild conditions. Various techniques are used for partial methane oxidation at low temperatures, such as photocatalysis, electrocatalysis, biocatalysis, and chemical catalysis [9]. The energy potential of methane is restricted by the input energy required for the breakdown of the C–H bond. Therefore, most of the methane conversion depends on thermochemical activation, which is a highly endothermic process (Figure 3A). In the photoelectrochemical (PEC) system, when light interacts with a photoanode, it causes the excitation of an electron to the conduction band, leaving the positive hole behind in the valance band. The positive hole oxidizes a methane molecule to the oxygenated product while the electron is transferred to the cathode via external circuit for the production of hydrogen gas (Figure 3B). This PEC system is distinguished from the photocatalyst (PC) system in which photocatalyst particles are dispersed in the medium or the electrochemical (EC) system in which an electrocatalytic electrode works without any incident light. Therefore, value-added chemical synthesis from methane utilizing solar light may achieve environmentally friendly synthetic pathways and reduce energy consumption, compared to the thermal oxidation process at high temperatures.

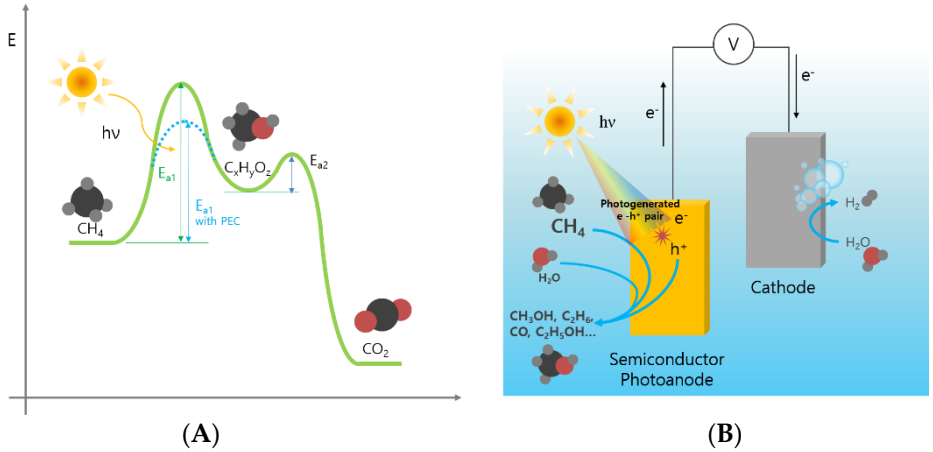

(**A**) (**B**)

Figure 3. Schematic energy diagram of methane oxidation with a photocatalyst (**A**) and photoelectrochemical system (**B**).

Although PEC methane oxidation has several advantages (controllable selectivity and rate by applied potential, tunability of electrode with co-catalyst, and easy design of device-type cells), PEC methane oxidation shows poor efficiency and selectivity compared to other methane oxidation methods, including photocatalytic and electrochemical methods. Basically, in PEC methane oxidation, a semiconductor/liquid (in this review, the liquid will be an aqueous solution) junction is formed at the semiconductor/electrolyte interface. Since the Fermi level of semiconductor (E_F) and chemical potential of electrolyte (chemical species) are at equilibrium, the energy band of semiconductor becomes the 'band-bending' state. The photo-generated electron–hole pairs are separated, and the electrons and holes are transported to the electrolyte/semiconductor interface and back contact under light-illumination conditions. Holes at the interface can activate chemical species (e.g., methane). The energy level of the valence band maximum (VBM) should be more positive than the standard redox potential of methane oxidation. Various semiconductor materials have a sufficient positive VBM, as shown in Figure 4. In addition, the conduction band minimum (CBM) does not directly affect the PEC oxidation reaction in n-type semiconductor materials, but it is desirable that the CBM of the semiconductor electrode should have a more negative energy level than 0 V vs. RHE ($E^{\circ}_{H+/H2}$). The suitable CBM and VBM levels of semiconductors spontaneously enable the full reaction (CH_4 methane oxidation at the photoanode and hydrogen evolution reaction at the cathode) under light-illumination conditions. Table 1 shows the standard redox potentials of the CH_4 oxidation reactions.

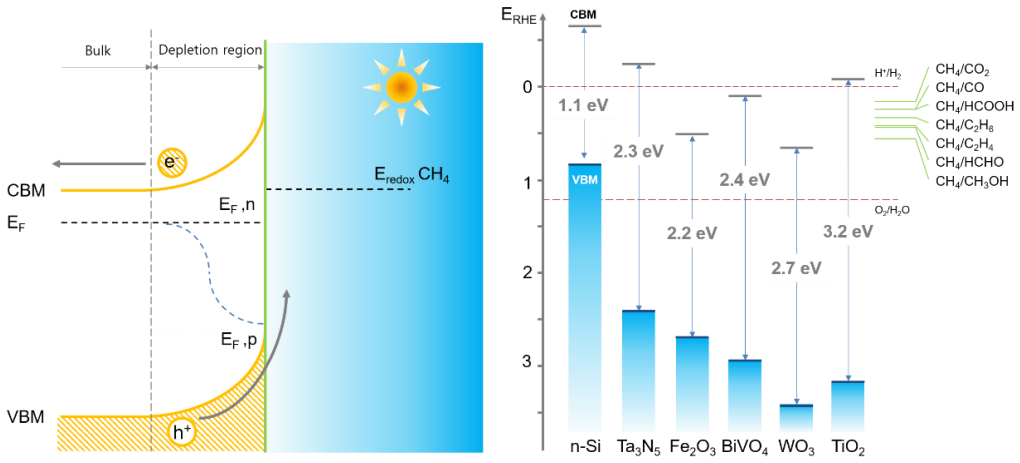

Figure 4. Solid/liquid junction at the semiconductor/electrolyte interface and band diagram of several semiconductor materials [10].

Table 1. Possible methane oxidation reactions along with standard electrode potentials.

Reaction	E (V) vs. RHE
$2H_2O\ (l) \rightarrow O_2\ (g) + 4H^+\ (aq) + 4e^-$	1.23
$CH_4\ (g) + 2H_2O\ (l) \rightarrow 2CO_2\ (g) + 8H^+\ (aq) + 8e^-$	0.17
$CH_4\ (g) + H_2O\ (l) \rightarrow CO\ (g) + 6H^+\ (aq) + 6e^-$	0.26
$CH_4\ (g) + H_2O\ (l) \rightarrow HCOOH\ (aq) + 6H^+\ (aq) + 6e^-$	0.26
$2CH_4\ (g) \rightarrow C_2H_6\ (g) + 2H^+\ (aq) + 2e^-$	0.35
$2CH_4\ (g) \rightarrow C_2H_4\ (g) + 4H^+\ (aq) + 4e^-$	0.44
$CH_4\ (g) + H_2O\ (l) \rightarrow HCHO\ (aq) + 4H^+\ (aq) + 4e^-$	0.46
$CH_4\ (g) + H_2O\ (l) \rightarrow CH_3OH + 2H^+\ (aq) + 2e^-$	0.58

Moreover, the bandgap is an important factor that determines the light-harvesting efficiency of the photoelectrode. Since ultraviolet light is only 1% of solar radiation, materials that can utilize the visible light region are strongly recommended for achieving high solar-to-chemical (STC) conversion efficiency. Based on these factors, screening suitable semiconductor materials can be the initial step for the rational initiation of PEC

methane oxidation research. Therefore, semiconductor materials that have been reported for PEC methane oxidation are discussed thoroughly in this review. Table 2 summarizes the semiconductor materials and their methane oxidation efficiencies.

Table 2. Comparison of different PEC methane oxidation systems.

Materials	Morphology	Preparation Method	Photo current Density ($mA \cdot cm^{-2}$)	Applied Potential	Light Intensity ($mW\ cm^{-2}$)	Light Source	Electrode Area (cm^2)	Methane Pressure (Atm)	Resction Mechanism	Faradaic Efficiency (%)	Product Rate	Electrolyte	Ref.
TiO_2	Nanotubes array	Anodizing	0.54	0.8 V_{RHE}	100	Hg (Xe) lamp (100 $mW \cdot cm^{-2}$)	0.23	1	Free radical	HCOOH (16%), CO_2 (72%), O_2 (12%)	-	0.05 M H_2SO_4	[11]
TiO_2	-	Atomic layer deposition	0.158	0.6 V_{RHE}	0.1	UV lamp (254 nm)	1	1	M-C σ bond	CO (52%), CO_2 (11%), O_2 (37%)	-	1 M NaOH (pH 3.3)	[12]
WO_3	Nanoplate	Hydrothermal	4	0.7 V_{RHE}	100	Xenon lamp (simulated solar light, 100 $mW \cdot cm^{-2}$)	1	-	Free radical	$HOCH_2CH_2OH$ (23.9%), C_2H_6 (2.1%), CH_3OH (2.3%), CO (4.3%), O_2 (63.5%)	0.47 $\mu mol \cdot cm^{-2} \cdot h^{-1}$	0.1 M Na_2SO_4	[13]
WO_3	Nanoparticle	Solution-based dip coating	4.2	1.2 V (two-electrode system)	6.8	3-W blue light LED lamps	16	1	-	C_2H_6 (12%), CO_2 (75.3%), CO (6.3%), O_2 (0.8%)	0.15 $\mu mol \cdot h^{-1}$	-	[14]
ZnO	Nanowire array	Hydrothermal	0.22	1 $V_{Ag/AgCl}$	100	Xe lamp (simulated solar light, 100 $mW \cdot cm^{-2}$)	10	1	Free radical	CH_3OH (11.69%)	0.571 $\mu mol \cdot min^{-1}$	0.05 M Na_2SO_4	[15]
ZnO/Au	Nanowire array	Hydrothermal	0.35	1 $V_{Ag/AgCl}$	100	Xe lamp (simulated solar light, 100 $mW \cdot cm^{-2}$)	10	1	Free radical	CH_3OH (32.11%)	1.407 $\mu mol \cdot min^{-1}$	0.05 M Na_2SO_4	[15]

2.1. TiO_2

TiO_2 is the most widely used photocatalytic material. Although TiO_2 has a wide bandgap (3–3.2 eV), its excellent electron and hole lifetimes enable high light-harvesting efficiency. For this reason, many researchers have reported CH_4 oxidation using TiO_2-related photocatalysts and PEC cells. Kadosh et al. [11] demonstrated the partial oxidation of methane via the PEC method, using TiO_2 nanotube arrays as a photoanode in acidic media, under ambient conditions. The major product, CO_2, was obtained along with trace amounts of other oxygenated products such as HCOOH, CO, and C_2H_6. In addition, O_2 was formed as a side-product, and its Faradaic efficiency (η_{FE}) increased with increasing applied potential. The current response of TiO_2 was higher in the presence of CH_4 than in its absence. The TiO_2 photoanode exhibited a higher η_{FE} toward CO_2, compared to formic acid (72% and 16%, respectively) due to the over-oxidation of methane [11]. Moreover, owing to its suitable band position, TiO_2 enables photo fuel cell operation with a Nafion 117 membrane and Pt/C under light illumination. A power density of 69 $\mu W \cdot cm^{-2}$ was obtained at a CH_4 concentration of 100%. On the other hand, Li et al. [12] demonstrated that the PEC oxidation of CH_4 on TiO_2 in NaOH aqueous electrolyte selectively produces CO, with carbonate as a by-product, at ambient temperatures. At a low voltage (~0.05 $mA \cdot cm^{-2}$ at 0.4 V vs. RHE), CO was obtained with a selectivity of 81.9%. The CH_4 oxidation on TiO_2 was initiated with the photoexcitation of electrons from O^{2-} to Ti^{4+}, to form $^{-\bullet}O–Ti^{3+}$, following which the $O^{\bullet -}$ oxidized CH_4 by abstracting hydrogen, to become $Ti–O–CH_3$.

The whole CH_4 oxidation process was synergistically controlled by the two adjacent Ti sites on the TiO_2 photoanode. The selectivity of the oxygenated product strongly depended on the TiO_2 surface state, with the Ti^{3+} species favoring the transition from C=O–Ti to O=C–Ti, which results in the formation of CO. Without the Ti^{3+}-assisted switching mechanism, CH_4 was selectively oxidized to CO_2. Electron paramagnetic resonance (EPR) studies showed that TiO_2 deposited through atomic layer deposition had a high concentration of Ti^{3+} active sites and exhibited superior catalytic activity, while the commercial titania (anatase and P25) had a low concentration of Ti^{3+}, producing a considerably small amount of CO. The Ti^{3+} site is critical in the CO synthesis route, because it assists in the formation of Ti^{3+}-C bonds. Otherwise, the Ti-O-C structure would result in the formation of carbonates. Furthermore, computational analyses showed that CO production is thermodynamically more favorable than over-oxidation (carbonate). Additionally, the selectivity for CO can be optimized by adjusting the applied voltage. The higher the applied voltage, the lower the CO selectivity, and vice versa [12]. The low pH of the electrolyte can be helpful in suppressing competitive reactions and oxygen evolution reactions (OERs). As mentioned above, the main limitation of TiO_2 is the absorption of light only in the UV region, owing to its wide bandgap. This limited light absorption is one of the reasons for the low photocurrent density (*J*). Therefore, bandgap tuning of TiO_2 may be required to increase the light absorption by doping transition metals (Fe^{2+}, W^{+3}, etc.) or anion exchange with N^- or S^{2-}. In addition, suppression of the competitive reaction (OER) is very important. Li et al. [12] suggested that Ti^{3+} plays a crucial role in increasing the selectivity of the methane oxidation reaction. Therefore, controlling the density of Ti^{3+} atoms by oxygen vacancy generation can be helpful.

2.2. WO_3

A single PEC cell with WO_3 cannot be operated in the absence of external bias, because of the CBM position of WO_3 (0.6 V vs. RHE) [16]. However, monoclinic WO_3 has been widely studied for PEC water oxidation, because it has a visible light-absorbable bandgap (2.4 eV).

According to Ma et al. [13], •OH is important for photocatalytic CH_4 activation. The adsorption behaviors of •OH on the (010), (100), and (001) facets of monoclinic WO_3 were studied using density functional theory (DFT). The surface structure of WO_3 had the smallest adsorption energy for •OH on the (010), (100), and (001) facets. The adjacent •OHs exhibited surface adsorption energies of −1.742, −1.826, and −1.935 eV on the (010), (100), and (001) facets, respectively, indicating strong adsorption of •OH on the twinning atoms of W on all three facets. However, each facet exhibited distinct •OH-adsorption behavior. At the (001) and (100) facets, both the •OH groups were close enough to form H_2O and surface-bonded oxygen via hydrogen bonds, thereby limiting their reactivity. In contrast, hydrogen bonds between the surface-adsorbed •OH on the (010) facets were difficult to form, because of the wide distance (3.342 Å) between two adjacent •OH groups. Thus, the surface adsorbed •OH at the (010) facets, resulting in the removal of the H atom from CH_4, and generation of $\bullet CH_3$. $\bullet CH_3$ reacted with •OH and $\bullet CH_3$ to form CH_3OH or C_2H_6. The highly reactive •OH further reacted with the produced CH_3OH, resulting in the formation of hydroxymethyl radicals. The twinning characteristics on the (010) facets of WO_3 allow the easy coupling of hydroxymethyl radicals with each other and the formation of C-C bonds, resulting in the formation of ethylene glycol at a production rate of 0.47 $\mu mol \cdot cm^{-2} \cdot h^{-1}$ at 1.3 V (RHE) [13].

In addition, product selectivity depends on methane solubility. The solubility of methane in 1.0 M NaOH is 1 $mmol \cdot kg^{-1}$. To cope with the low solubility of methane in water, Amano et al. [14] demonstrated PEC processes in a triple-phase boundary system, to convert CH_4 to C_2H_6 using WO_3, with a bandgap of 2.7 eV that absorbs blue light (Figure 5) [14]. The electron–hole recombination was reduced by the applied potential (1.2 V). The WO_3 semiconductor was deposited on Ti microfibers, to efficiently transport photo-excited electrons and holes, to oxidize CH_4 into $\bullet CH_3$, thus accelerating the

formation of ethane. The concentration of CH_4 significantly affected the photocatalytic activity. At 10% CH_4 in the reactor, the OER was prominent for the production of O_2. However, water oxidation was suppressed upon increasing the concentration of methane up to 97%, resulting in an increased ethane selectivity of 54%, with 0.1% methane conversion [14]. When the PEC reaction is carried out under aqueous electrolyte conditions, photo-generated OH• is not only the oxidant for CH_4 but also an intermediate of O_2. Therefore, the selective suppression of OH• coupling is directly related to achieving high selectivity in methane oxidation. In conclusion, these studies provide insight into selective CH_4 oxidation by WO_3, especially in terms of facet control, which can be a good strategy for PEC methane oxidation. In addition, for triple-phase PEC cells, the side reaction is negated because of the low concentration of H_2O. However, this does not suppress the over-oxidation of methane. Lastly, WO_3 is predicted to be a material with great potential for PEC methane oxidation, since it produces H_2O_2 or OH• during PEC conditions [17], and these peroxide species can be used as strong oxidants for methane oxidation.

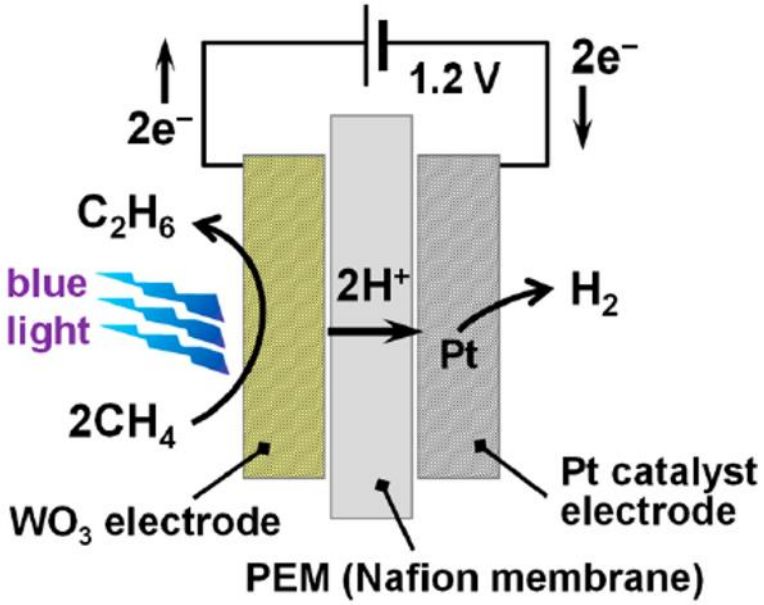

Figure 5. Membrane electrode assembly for PEC CH_4 activation [14]. Copyright 2019, American Chemical Society.

2.3. ZnO

Liu et al. [15] compared ZnO and Au-decorated ZnO nanowire arrays for PEC methane oxidation to methanol under ambient conditions. The ZnO photoanode exhibited photocatalytic activity toward methane oxidation. However, the decoration of Au on ZnO further enhanced its catalytic activity by expanding the optical absorption in the visible spectrum via surface plasmon resonance. The co-catalyst, Au, lowered the activation energy and facilitated methane oxidation by avoiding charge recombination at trapping sites and providing the active site. Au-decorated ZnO exhibited a Faradaic efficiency of 32.11%, which is three times higher than that of the ZnO catalyst [15]. Hexagonal ZnO is also a wide bandgap material (3–3.1 eV), so only UV light can be utilized in its case. The above result suggests that the combination of plasmons with wide bandgap semiconductors can overcome light absorbance limitations.

2.4. Potential Semiconductor Materials

Fe_2O_3 (hematite) has a suitable VBM for methane oxidation and an ideal bandgap (2.1–2.2 eV) for visible light absorption. Fe_2O_3 is very stable during the PEC oxidation reaction with a wide pH range, regardless of the acid or base [18]. $BiVO_4$ also has a significant potential for methane oxidation because it is widely used for various oxidation

reactions, not only for water oxidation, but also for organic chemical oxidation [19]. $BiVO_4$ has a bandgap of 2.4 eV. Moreover, it is stable during the PEC reaction in a neutral pH electrolyte. In addition to metal oxide semiconductors, Ta_3N_5 and n-Si can be utilized for PEC methane oxidation. Ta_3N_5 also has a suitable band position and bandgap, while n-Si has a narrow bandgap (1.1 eV) that utilizes solar light till the near-IR range. In particular, n-Si has unique properties compared to other materials, and the CBM of n-Si is located between the standard redox potential of H_2O and CH_4 oxidation potential (CH_4/C_2H_6). Therefore, water oxidation is thermodynamically limited at the n-Si photoelectrode under methane oxidation conditions. Lastly, other materials such as metal chalcogenide, carbon-derived materials, C_3N_4, metal carbide can be candidates for PEC methane oxidation because these materials have been reported to show the photocatalytic activity for partial oxidation of methane in the PC system [2].

3. Mechanistic Insights for High Selectivity during Methane Oxidation

Unlike photocatalytic and electrochemical methane oxidation, only a few reports have been published on PEC methane oxidation. Therefore, its reaction mechanisms can be adapted from thermal catalytic, electrochemical, or photocatalytic reactions. Both photocatalytic and PEC reactions are based on similar basic principles. However, the detailed mechanisms are quite different. In the photocatalytic system, all the reactions occur at the dispersed photocatalyst material interface, whereas in the PEC system, the reduction and oxidation reactions occur at different electrodes. In photocatalytic methane oxidation, oxidants or their precursors, such as OH-, O_2, or H_2O_2, have been reported to be activated to form radicals by photo-generated electrons. These activated radicals and photo-generated holes play crucial roles in methane oxidation. On the other hand, in the PEC system, the excited electrons are transported to the counter electrode, where they are utilized for the hydrogen evolution reaction (Figure 6). The independence of the redox reaction should be considered when designing a PEC methane oxidation system.

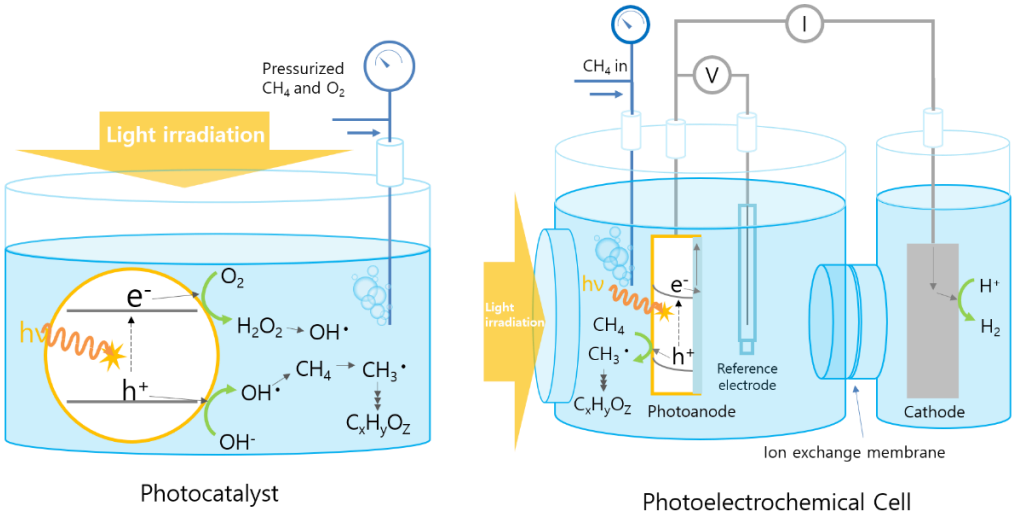

Figure 6. Comparison of the methane oxidation mechanisms of the photocatalyst and photoelectro chemical cell systems.

In the PEC system, methane can be activated by either direct or indirect pathways (Figure 7). In the direct pathway, the CH_4 molecule interacts with the catalyst and forms a chemical bond. This bond can be the M-C sigma bond formed by CH_4 with the metal center of the oxide catalyst [20]. The H atom in CH_4 can also form an O-H bond with the oxygen atom of the oxide catalyst [8]. This type of activation, which is generally found in gas-phase systems, is also possible in an electrochemical and PEC system with an aqueous electrolyte [21]. On the other hand, the indirect methane activation is carried out by an electron shuttle (e.g., $Pt(bpy)Cl_2$) or unstable species (OH•)), without a direct interaction

between CH_4 and the catalyst (Figure 7). The mechanism by which radical species are involved in indirect CH_4 oxidation is generally known to be a radical mechanism.

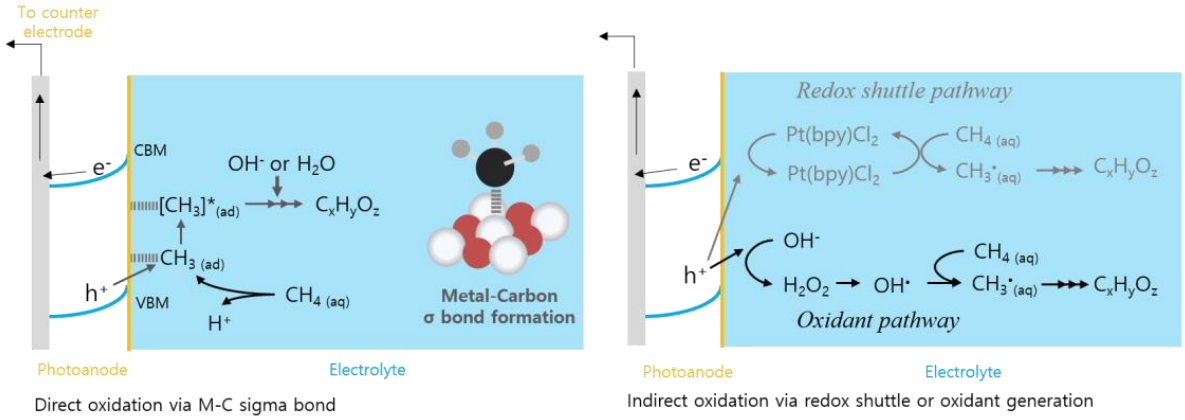

Figure 7. Direct and indirect methane oxidation mechanisms for a photoelectrochemical cell.

3.1. Direct Oxidation: Co-Catalyst Approach

The combination of a co-catalyst is a promising method for methane oxidation, to control the selectivity and suppress the oxygen evolution at the photoelectrode surface. The interaction between the intermediates (CH_3* and OH*) and the catalyst surface mainly determines the reaction pathway. This approach is considered in the computational studies of electrochemical methane oxidation. Although many experimental studies on electrochemical methane oxidation have been reported, only a few computational studies have provided comprehensive details on the reaction mechanism. Platinum is an extensively studied catalytic material for the full oxidation of CH_4 to CO_2. Boyd et al. [22] provided a combination of computational and experimental studies, to understand the mechanism of oxidation reactions and the factors influencing the selectivity and catalytic activity on the Pt surface. Although this research does not focus on the partial oxidation of CH_4 to oxygenated products, the findings may be utilized to explain the selectivity issues of Pt and other transition metals. The experimental and DFT calculations show that methane activation is the rate-determining step, which depends to a certain extent on the applied voltage. The most stable intermediate on the Pt surface during the partial oxidation of methane is CO. A scaling plot of CO adsorption energy and activation energy of methane indicates that the transition metals with lower CO adsorption energy will have a high energy barrier for the activation of methane, resulting in decreased overall reaction kinetics. In addition, the reaction rate can also be lowered by strong CO adsorption on the metal surface, which can block the active site and cause catalyst poisoning. This could be avoided by increasing the applied potential, which results in the over-oxidation of CH_4 to CO_2. The oxygenated products could be successfully formed by breaking the scaling relationship between the CO adsorption energy and activation energy of CH_4.

Table 1 shows that water is involved in electrochemical methane oxidation. Both water and methane are oxidized at the positive electrode of an electrochemical cell. As a result of water oxidation, reactive oxygen species are generated on the surface of the catalyst (reactions (1) and (2)).

$$H_2O + * \rightarrow OH^* + (H^+ + e^-) \quad (1)$$

$$OH^* \rightarrow O^* + (H^+ + e^-) \quad (2)$$

Arnarson et al. [23] reported that the presence of oxygen active species on the catalyst surface facilitated the abstraction of hydrogen from CH_4 and accelerated the rate of methane oxidation. They investigated the surfaces of monolayer MX-enes (two-dimensional transition metal nitrides and carbides) and transition metal oxides using DFT simulations and predicted that the rate of methane oxidation was low for catalyst materials on which water

splitting was a bottleneck process. They proposed promising materials such as SnO_2, TiO_2, and PtO_2 for methane oxidation, owing to the low energy barrier for the formation of surface-adsorbed oxygen species (O* and OH*). Furthermore, they estimated the rate of methane oxidation, considering the availability of oxygen active species on the surface of the catalyst and revealed that increasing the applied potential significantly reduced the energy barrier for methanol formation. They also compared the rate of methanol formation with the OER for O* binding energy and showed that abundant oxygenated species were formed on the surface by increasing the applied potential, which facilitated the OER. Consequently, the rate of methanol formation decreased and O_2 was formed as a major product. Although OER intermediates facilitate methane oxidation by providing the necessary oxygenated species, they also provide a competitive reaction at high potentials. Therefore, an efficient catalyst material must increase the rate of methane oxidation by preserving the OER intermediates at higher potentials.

Luo et al. [24] studied several metal porphyrins (MN_4, where M = Rh, Ru, Co, Mn, Fr, Cr, Ir, and Os) implanted in graphene for electrochemical methane oxidation to methanol and other light alkanes. Previous studies have shown that this class of materials is an active OER catalyst. Hence, they can be utilized to produce active surface oxygen for methane activation. Additionally, these materials have separate active metal centers, which restrict access to reactive oxygen species and inhibit the over-oxidation of CH_4. The authors prepared a Pourbaix diagram that can be used to determine active oxygen species and oxidation products at a potential of 0–2.5 V between pH 0–14. They concluded that the continuous formation of oxygenated products requires careful potential and pH control, and even minute changes in these reaction parameters might stop methane oxidation or cause over-oxidation. The methane oxidation and OERs compete with each other during electrocatalysis, owing to the variation in the energetics of the reaction intermediates. Arnason et al. [23] calculated the Gibbs free energy for each intermediate of both reactions occurring on MX-enes and various metal oxides. In both reactions, the hydroxide groups are the first intermediate to be absorbed on the surface of the catalysts, which are then converted into active oxygen atoms (O*) by the dehydrogenation process. The reaction of O* with methane is considered a bottleneck step in methane oxidation, because O* also reacts with water to generate O_2. At the open-circuit voltage, the Gibbs free energy for the oxidation of methane (pink) and the third step of the OER (blue) are shown for several metal oxides in Figure 8. Depending on the endergonicity of each step, both reactions required different anodic potentials. The lower the endergonicity, the more easily the reaction will proceed. Methanol could be preferentially produced with a lower Gibbs free energy than O_2. Accordingly, the most promising catalysts for the oxidation of methane to methanol are SnO_2, TiO_2, V_2O_5, RhO_2, and PtO_2.

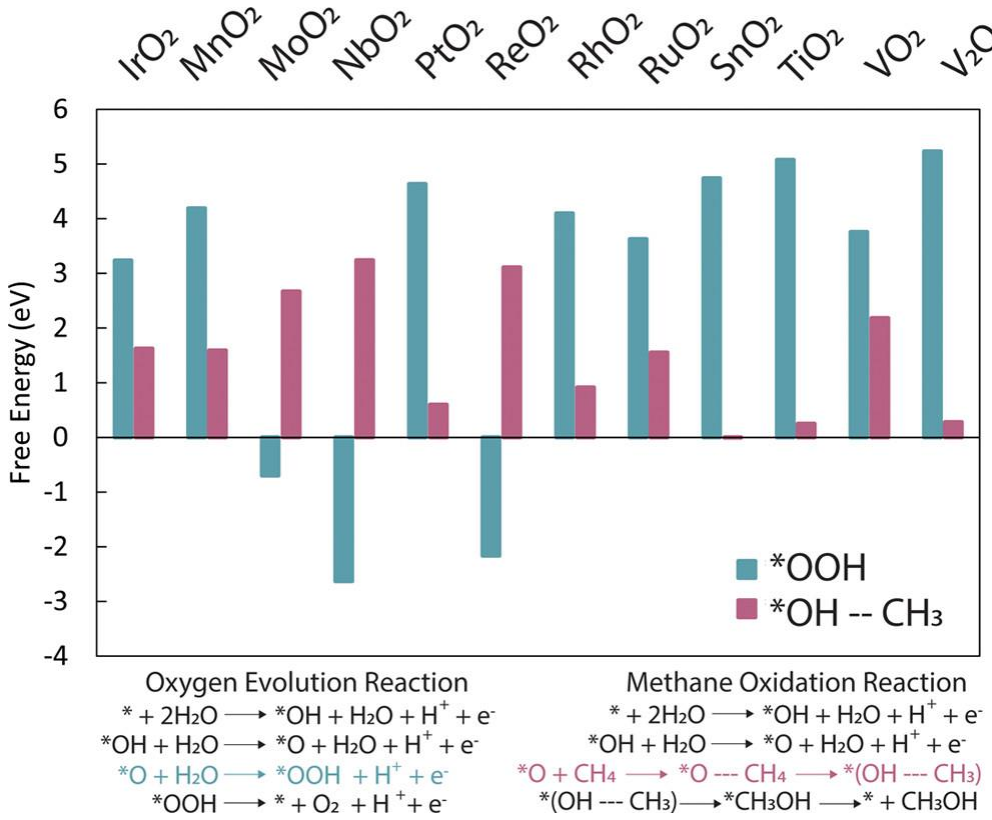

Figure 8. Free energy for the 3rd step of OER and methane oxidation on various metal oxides [25]. The "*" represents the active sites of the catalyst. Copyright 2020, American Chemical Society.

Lee et al. [26] reported the formation of methanol on V_2O_5/SnO_2 in a ceramic proton exchange membrane electrode assembly with 88.4% selectivity and 0.03% conversion. The high selectivity of methanol was attributed to the partially reduced species (V^{4+}) in V_2O_5, which promoted the formation of active oxygen species ($O^{\bullet -}$ and $O_2^{\bullet -}$). These species can chemisorb and partially oxidize methane to produce methanol. The authors suggested that partial and complete oxidation of methane occurs through different reaction pathways. They proposed that the partial oxidation of methane to methanol occurs via $O^{\bullet -}$ and $O_2^{\bullet -}$ active oxygen species. However, the complete oxidation of methane to CO_2 was facilitated by the highly active OH* surface sites. Heo et al. [27] and Yamagata et al. [28] proposed the same reaction pathway for the over-oxidation of methane. The efficiency of the cell can be increased by suppressing the formation of CO_2, by reducing the number of OH* sites. However, V_2O_5 requires different supports because SnO_2 causes over-oxidation of methane to CO_2 [26]. In summary, a co-catalyst for PEC methane oxidation in aqueous solution should have poor OER activity and high activity for methane oxidation, to suppress competitive OER. The candidates for PEC methane oxidation can be PtO_2, V_2O_5, IrO_2, and RuO_2. However, the junction between these materials and photoanode materials should also be considered for efficient hole transportation.

3.2. Indirect Oxidation: PEC Production of Oxidant

Although there are no reports on the indirect photo-oxidation of methane via PEC cells, some insights from thermal and electrochemical CH_4 oxidation results can be adopted for PEC cells. Several homogeneous catalysts, such as transition metal complexes, have been reported to be used for methane activation [20]. These homogeneous catalysts transfer electrons and holes between the oxidant and methane, to activate the C-H bond for methane oxidation. Kim et al. [29] demonstrated the electrochemical regeneration of Shilov salt Pt^{IV}, in which the ratio of Pt^{III}/Pt^{IV} in the electrolyte was sustained during methane activation (Figure 9). This strategy provides steady methane oxidation, with 70% methanol selec-

tivity, by controlling the $Pt^{II/IV}$ ratio throughout the oxidation cycle. A similar approach was also used by O'Reilly et al. [30], for the electrochemical regeneration of Pd catalysts through Faradaic and non-Faradaic pathways for methane oxidation [30]. Therefore, PEC regeneration of the redox shuttle is possible with a suitable photoanode and redox couple.

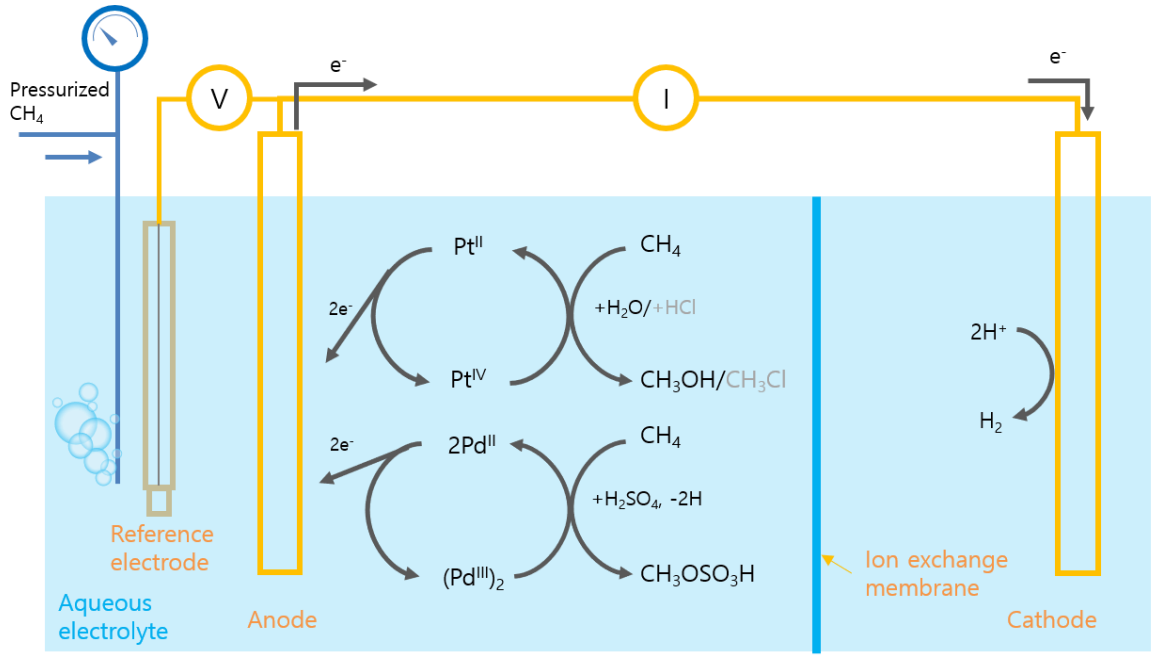

Figure 9. Schematic diagram of functionalization of methane with an electrochemical redox shuttle complex [29,30].

Previous studies have reported a PEC setup with a redox shuttle system for different chemical syntheses, both reduction and oxidation of target molecules. For example, Cha et al. [31] demonstrated the oxidation of 5-hydroxymethylfurfural with a $BiVO_4$ photoanode and a TEMPO redox shuttle. Therefore, the combination of photoanode materials such as $BiVO_4$, WO_3, and Ta_3N_5, and selective transition metal complexes (Pt, Pd, Eu, V, etc.) may enable the PEC-mediator oxidation of methane for future research.

On the other hand, the radical mechanism is widely adopted in photocatalytic systems. Water, H_2O_2, or OH^- is oxidized on a semiconductor surface to form radical species that are used as oxidants for methane oxidation [32]. Similarly, PEC radical or oxidant generation is an important strategy that can be used for methane oxidation. Notably, highly selective PEC H_2O_2 production by $BiVO_4$, WO_3, and other semiconductor materials has been reported. H_2O_2 is a strong oxidant that is widely used for thermal CH_4 oxidation. Therefore, PEC H_2O_2 production under methane-saturated electrolyte conditions is a potent suggestion for methane oxidation. Recently, it has been reported that bicarbonate (or carbonate) ions improve the methane oxidation activity of electrocatalysts.

Lee et al. [33] reported a CuO/CeO_2 electrocatalyst for methane oxidation catalysts in an electrolyte containing CO_3^{2-} ions. Under anodic potential conditions, CO_3^{2-} ions can be oxidized to active radical species. According to Sayama et al. [34] (bi)carbonate ions form bidentate peroxospecies, which decompose into the radical form. The radicals and water molecules react with H_2O_2 in an aqueous electrolyte, in the presence of metal oxide electrocatalysts such as SnO_2, TiO_2, and $BiVO_4$ [35]. Therefore, the combination of a photoanode and CH_4-saturated bicarbonate electrolyte can serve as a potent candidate system for indirect PEC methane oxidation. In addition, Murcia-López et al. [36] reported increased methanol selectivity of $BiVO_4$ photocatalysts in the presence of nitrite ions (NO_2^-), which act as a UV filter, as well as, a hydroxyl radical scavenger [36].

4. Other Factors That Affect Methane Oxidation

Apart from the catalyst materials and oxygen sources, several other factors can affect the PEC methane oxidation performance. This section summarizes the literature on electrolytes, partial pressure of methane, and operating temperature. These variables can significantly affect the product selectivity and overall energy efficiency of PEC methane oxidation.

Until now, PEC methane oxidation has been examined in various electrolytes such as solid-state ionic liquids [37], solid-state electrolytes [38], organic electrolytes [8], and aqueous electrolytes [8]. In a liquid-phase electrochemical system, electrolytes play an important role by providing a reaction environment that facilitates charge transfer to the electrodes. The oxidation of methane at the electrode/electrolyte interface is highly sensitive to pH, which can control the overall kinetics of methane electrocatalysis. Methane oxidation has been performed in acidic, neutral, and basic electrolytes. It is very difficult to obtain a high product yield during methane oxidation in a conventional electrocatalytic system, because of the extremely low solubility of methane (<22.7 $mg \cdot L^{-1}$) in acidic, neutral, and basic aqueous media. However, Santos et al. [39] successfully oxidized methane to methanol in an alkaline anion-exchange membrane fuel cell using a Pt/C electrocatalyst. The high yield of methanol was attributed to the low availability of protons near the electrode-electrolyte interface in the basic medium, which facilitated methane oxidation. In contrast, Amenomiya et al. [40] reported that OH^- exhibited very low activity in the deprotonation of methane under normal conditions. These oxidation kinetics can be significantly improved by using carbonate-based electrolytes, in which charged oxygen atoms enhance the reaction enthalpy. Therefore, carbonate-based electrolytes are preferred for methane oxidation, over alkaline systems. Moreover, metal oxides such as NiO [41], Co_3O_4 [42], and $NiCo_2O_4$ [43], are more stable in alkaline media or methane oxidation. Acidic media have been reported to oxidize methane through catalytic cycles using Pd and Pt salts [30].

The operating temperature is an important and detrimental factor in the electrochemical oxidation of methane. Under mild reaction conditions, the kinetics of electrochemical methane oxidation are very slow, owing to the high activation energy required for the C-H bond in methane. Until now, electrochemical methane oxidation has been intensively investigated in an electrochemical cell with solid electrodes immersed in liquid-phase electrolytes, while purging methane in the liquid electrolyte at room temperature [6]. Hibino et al. [26] used a confined fuel cell-type reactor to study the effect of temperature on the partial electrochemical oxidation of methane to methanol. Initially, the reaction was carried out on a Pt/C anode supplied with a mixture of water vapor and methane. As the reaction temperature increased from 50 °C to 250 °C, the concentration of methane decreased, as evidenced by an increase in the current density. The main products of methane oxidation were CO_2 and O_2, whose concentrations decreased at higher temperatures, leading to excessive formation of CO_2, which was attributed to the high adsorption energy of CO. They also studied non-noble metal oxide catalysts with different supports, other than carbon, to improve the product yield toward CH_3OH and reported a 50% increase in methanol selectivity and 61.4% in Faradaic efficiency on V_2O_5/SnO_2 at 100 °C. Additionally, chronopotentiometry analysis showed that a high production of methanol was obtained at +900 mV. They concluded that highly dispersed vanadium species were partially reduced on the SnO_2 support and that the high catalytic activity of V^{4+} sites at +900 mV could be attributed to the formation of active oxygen species by means of anodic polarization of water vapors.

The metal/oxide interface also improves the redox and long-term stability of the catalyst by preventing the agglomeration of metal nanoparticles, which is caused by the lowering of the surface energy. Lu et al. [44] reported that a stiff metal/oxide interface is involved in the activation of CO_2 and inhibits coking in the electrochemical reforming of CH_4/CO_2. Zhu et al. [45] showed that the catalytic stability could be enhanced at elevated temperatures by the metal/oxide interface, which limited the formation of coke during the electrochemical oxidation of methane. In addition, the nanoscale metal/oxide interface

facilitates the transformation of O^{2-} to the active anodic interfaces, by accommodating the O^{-} ions. In addition to these reactive oxygen species on a suitable interface catalyst, the electrochemical pumping of O^{2-} ions from the cathode to the anode is not only involved in the direct oxidation of methane, but also promotes gaseous selective coupling to produce ethylene.

Regarding the partial pressure of methane, high pressure is more likely to increase the solubility of methane in aqueous electrolytes, which leads to high oxidation current densities. The product selectivity is significantly affected upon adjusting the absolute and partial pressures of CH_4, which can alter the intermediates of methane oxidation, binding energies of adsorbed oxidants, and relative surface coverage of the catalyst [46]. Nevertheless, only a few studies have reported on the electrochemical oxidation of methane under pressurized systems. O'Reilly et al. [30] reported the electrochemical oxidation of Pd^{II} salts in hot concentrated H_2SO_4 solutions, to produce methanol precursors, such as methane sulfonic acid (CH_3SO_3H) and methyl bisulfate (CH_3OSO_3H). The increase in the pressure of methane in the electrochemical cell, from 100 to 500 psi, significantly increased the anodic current densities at 1.8 V. The same relationship was found between the current density and the partial pressure of methane, when the reaction temperature was lowered to 100°C. However, the negligible anodic current densities beyond 1.5 V indicated that high-valent species were utilized in the oxidation of methane. Most studies on CH_4 oxidation were conducted under pressurized conditions (1–100 bar) in thermal or photocatalytic systems, because the solubility of methane in aqueous solution is only ~1 mM under ambient pressure conditions [47]. Increasing the partial pressure of CH_4 is one of the direct ways to increase the product yield and suppress the OER.

In addition, light intensity has a significant effect on methane oxidation in the PC system. Wei et al. investigated the effect of light intensity on the photocatalytic performance of Ga_2O_3/AC composite for methane oxidation [48]. Wei et al. reported that the oxidation of methane is directly proportional to the intensity of the irradiation, indicating that light plays a major role in CH_4 oxidation via PC system. However, In PEC system, the standardized light source condition (1 sun, 100 $mW{\cdot}cm^{-2}$ with AM 1.5) is strongly recommended for photoelectrochemical measurements. The relationship between light intensity and product selectivity in PEC methane oxidation is not clearly revealed.

5. Effect of Catalyst Structure on Reaction Selectivity

It cannot be denied that the structure and phase of the electrocatalysts are closely related to the catalyst activity. In addition to the bulk structure, which can be determined using X-ray diffraction, the local crystal structure and electronic properties can be determined using high-resolution transmission electron microscopy, Raman spectroscopy, and X-ray photoelectron spectroscopy, and can serve as critical factors that affect the catalytic activity. Iridium oxide is an ideal OER catalyst that exhibits various catalytic activities, owing to its amorphous or crystalline form [49]. Similarly, Liang et al. [50] reported that certain facets of IrO_2 can cause methane oxidation [50]. Another study by Ma et al. [42] showed that specific facets on the surfaces of Pt catalysts are also involved in the oxidation of CH_4 to CO [42]. In bi-functional catalytic materials, the interaction of the surfaces of different materials with several exposed facets may cause synergistic catalytic effects. Notably, bi-functional materials are unstable under a high applied potential; thus, their structural analysis must be performed before and after the reaction.

Notably, the characterization of photoelectrodes under in situ conditions will be very important to reveal the reaction mechanism. Li et al. [12] and Ma et al. [13] detected H_3C-O-M intermediates on Ti^{3+} and different WO_3 facets using in situ Raman spectroscopy and in situ diffuse reflectance infrared Fourier transform spectroscopy, respectively. These intermediates were formed by unstable radical species, which were detected using EPR spectroscopy, to gain a clear understanding of the reaction mechanism. These results provide clear evidence of CH_4 oxidation, which is carried out by means of a direct oxidation mechanism on these catalysts.

6. Activity Evaluation for PEC Methane Oxidation

While reporting the PEC methane oxidation performance, various values such as production rate, Faradaic efficiency, current density, power density, and selectivity for target molecules have been reported, but with low efficiency. Some meaningful criteria must be set to compare the efficiency of the photoelectrode. The ultimate goal of PEC methane oxidation is to convert solar energy to chemical energy, which can be represented in terms of STC efficiency, calculated using Equation (3).

$$\text{STC conversion efficiency } (\%) = \frac{\Sigma\, E^{\circ}_{Chemical} \times J \times \eta_{FE}}{P} \times 100\% \quad (3)$$

where $\Sigma\, E^{\circ}_{Chemical}$ is the standard potential of the methane oxidation reaction, J is the current density, η_{FE} is the Faradaic efficiency (i.e., current efficiency with which electrons carry out a desired electrochemical reaction) and P is the power density of the incident light.

The STC is only valid for a spontaneous operating cell with a two-electrode configuration. However, owing to the overpotential and thermodynamic restriction of the energy structure of semiconductor materials, many photoanodes have been studied with only half-cell configurations. Although the production rate ($\text{mol}\cdot\text{s}^{-1}$) can be a useful parameter to determine the activity of the photoelectrode, it is not recommended for the PEC system, because it is an electrode area-dependent value and not a specific value. The production rate per specific catalyst mass ($\text{mol}\cdot\text{g}^{-1}\cdot\text{s}^{-1}$) is not preferred for the PEC system, because electrode activity is generally estimated in terms of the area, rather than the mass of the semiconductor film. Therefore, J and η_{FE} at a specific applied potential value are strongly recommended as representative values for PEC methane oxidation activity. The Faradaic efficiency in (photo)electrochemistry is an identical concept to the selectivity in the chemical reaction. The selectivity and reaction rate of the photoelectrode can be easily deduced from the η_{FE} and J values (Equations (4)–(6)). In addition, the term 'selectivity' should be carefully used in this scenario, because there is a possibility of getting confused between selectivity (Equation (6)) and selectivity of CH_4 oxidation (Equation (7)).

$$\eta_{FE}\ (\%) = \frac{\text{target chemical (mol)}}{(J \times t/z \times F)} \times 100\% \quad (4)$$

$$\text{Reaction rate } (\text{mol}\cdot\text{s}^{-1}) = \frac{J \times \eta_{FE}}{z \times F \times 100} \quad (5)$$

$$\text{Selectivity } (\%) = \frac{\text{target chemical (mol)}}{\text{Total product (mol)}} \times 100\% \quad (6)$$

$$\text{Selectivity of } CH_4 \text{ oxidation } (\%) = \frac{\eta_{FE} \text{ of target chemical}}{\Sigma\, \eta_{FE} \text{ of all chemicals from } CH_4 \text{ oxidation}} \times 100\% \quad (7)$$

where z is the number of electrons transferred in the half-reaction of target chemicals, F is faraday constant, J is the current density, and t is a reaction time.

7. Conclusions and Future Perspectives

The PEC methane oxidation system, in which abundant methane can be transformed into value-added products using solar light, is considered as an ideal solution to replace the present oil-based chemical industry. However, the past and present PEC systems have been able to provide very low product yields, similar to those already observed in other direct chemical transformations of methane under mild conditions. In PEC methane oxidation, the most important aspect is the design of the photocatalyst, which can efficiently absorb solar light to generate charges for CH_4 oxidation. In this regard, the bandgap is an important factor in determining the light-harvesting efficiency of photoelectrodes. Since ultraviolet light is only 1% of solar radiation, materials that can utilize the visible light region are strongly recommended for achieving high STC conversion efficiency. Thus, substantial efforts are required to develop and adopt smaller bandgap materials with

suitable energy levels (e.g., WO_3, Fe_2O_3, $BiVO_4$, and Ta_3N_5), as well as, those incorporated with co-catalysts (e.g., Au, Ag, Pt, Pd, PtO_2, V_2O_5, IrO_2, and RuO_2), to reduce the energy barriers and enhance the electrical conductivity at the interface. Methane can also be oxidized by an indirect method in which an electron shuttle or unstable species activates the C-H bond without the direct interaction of CH_4 and the catalyst. The hydroxyl radical is an important intermediate in methane oxidation, which can be obtained by the in situ production of H_2O_2 by a photocatalyst. However, the high reactivity of •OH is not plausible for achieving high product selectivity during methane oxidation, and a controlled release of •OH is favorable. Optimizing these parameters may lead to the development of a highly efficient PEC methane oxidation system for CH_4. Other issues include the long-term stability of the photocatalyst and low selectivity of the targeted products. The long-term stability can be improved by engineering the interface of the heterostructure, which can not only minimize the agglomeration of the particles but also reduce coking on the catalyst. For this purpose, a single atom or a very low concentration of catalyst deposited on a suitable substrate might be a possible solution. On the other hand, the selectivity of the target product can be improved by means of a thorough investigation of the reaction mechanism using both computational and experimental methods. Other factors, such as the design of the PEC cell, temperature, pressure, electrolyte, and oxidizing agent affect the product selectivity. After resolving the critical issues on the target product yield, a techno-economic analysis on the PEC process considering the manufacturing cost of the PEC system, energy efficiency, product value, and separation cost can be conducted.

Author Contributions: Conceptualization, E.D.P.; writing—original draft preparation, A.M.; writing—review and editing, S.Y.C. and E.D.P.; supervision, project administration, and funding acquisition, E.D.P. All authors have read and agreed to the published version of the manuscript.

Funding: This work was supported by the C1 Gas Refinery Program through the National Research Foundation of Korea (NRF) funded by the Ministry of Science, ICT, and Future Planning (2015M3D3A1A01064899).

Conflicts of Interest: The authors declare no conflict of interest.

References

1. McFarland, E. Unconventional chemistry for unconventional natural gas. *Science* **2012**, *338*, 340–342. [CrossRef] [PubMed]
2. Li, Q.; Ouyang, Y.; Li, H.; Wang, L.; Zeng, J. Photocatalytic Conversion of Methane: Recent Advancements and Prospects. *Angew. Chem. Int. Ed.* **2021**. [CrossRef]
3. Hu, D.; Ordomsky, V.V.; Khodakov, A.Y. Major routes in the photocatalytic methane conversion into chemicals and fuels under mild conditions. *Appl. Catal. B* **2021**, *286*, 119913. [CrossRef]
4. Sher Shah, M.S.A.; Oh, C.; Park, H.; Hwang, Y.J.; Ma, M.; Park, J.H. Catalytic Oxidation of Methane to Oxygenated Products: Recent Advancements and Prospects for Electrocatalytic and Photocatalytic Conversion at Low Temperatures. *Adv. Sci.* **2020**, *7*, 2001946. [CrossRef]
5. Baek, J.; Rungtaweevoranit, B.; Pei, X.; Park, M.; Fakra, S.C.; Liu, Y.-S.; Matheu, R.; Alshmimri, S.A.; Alshehri, S.; Trickett, C.A.; et al. Bioinspired Metal–Organic Framework Catalysts for Selective Methane Oxidation to Methanol. *J. Am. Chem. Soc.* **2018**, *140*, 18208–18216. [CrossRef]
6. Mostaghimi, A.H.B.; Al-Attas, T.A.; Kibria, M.G.; Siahrostami, S. A review on electrocatalytic oxidation of methane to oxygenates. *J. Mater. Chem. A* **2020**, *8*, 15575–15590. [CrossRef]
7. Tomkins, P.; Ranocchiari, M.; van Bokhoven, J.A. Direct Conversion of Methane to Methanol under Mild Conditions over Cu-Zeolites and beyond. *Acc. Chem. Res.* **2017**, *50*, 418–425. [CrossRef]
8. Meng, X.; Cui, X.; Rajan, N.P.; Yu, L.; Deng, D.; Bao, X. Direct Methane Conversion under Mild Condition by Thermo-, Electro-, or Photocatalysis. *Chem* **2019**, *5*, 2296–2325. [CrossRef]
9. Zakaria, Z.; Kamarudin, S.K. Direct conversion technologies of methane to methanol: An overview. *Renew. Sustain. Energy Rev.* **2016**, *65*, 250–261. [CrossRef]
10. Sivula, K.; van de Krol, R. Semiconducting materials for photoelectrochemical energy conversion. *Nat. Rev. Mater.* **2016**, *1*, 15010. [CrossRef]
11. Kadosh, Y.; Korin, E.; Bettelheim, A. Room-temperature conversion of the photoelectrochemical oxidation of methane into electricity at nanostructured TiO_2. *Sustain. Energy Fuels* **2021**, *5*, 127–134. [CrossRef]
12. Li, W.; He, D.; Hu, G.; Li, X.; Banerjee, G.; Li, J.; Lee, S.H.; Dong, Q.; Gao, T.; Brudvig, G.W.; et al. Selective CO Production by Photoelectrochemical Methane Oxidation on TiO_2. *ACS Cent. Sci.* **2018**, *4*, 631–637. [CrossRef] [PubMed]

13. Ma, J.; Mao, K.; Low, J.; Wang, Z.; Xi, D.; Zhang, W.; Ju, H.; Qi, Z.; Long, R.; Wu, X.; et al. Efficient Photoelectrochemical Conversion of Methane into Ethylene Glycol by WO_3 Nanobar Arrays. *Angew. Chem. Int. Ed.* **2021**, *60*, 9357–9361. [CrossRef] [PubMed]
14. Amano, F.; Shintani, A.; Tsurui, K.; Mukohara, H.; Ohno, T.; Takenaka, S. Photoelectrochemical homocoupling of methane under blue light irradiation. *ACS Energy Lett.* **2019**, *4*, 502–507. [CrossRef]
15. Liu, J.; Zhang, Y.; Huang, Z.; Bai, Z.; Gao, Y. Photoelectrocatalytic Oxidation of Methane into Methanol over ZnO Nanowire Arrays Decorated with Plasmonic Au Nanoparticles. *Nano* **2018**, *14*, 1950017. [CrossRef]
16. Alexander, B.D.; Kulesza, P.J.; Rutkowska, I.; Solarska, R.; Augustynski, J. Metal oxide photoanodes for solar hydrogen production. *J. Mater. Chem.* **2008**, *18*, 2298–2303. [CrossRef]
17. Seabold, J.A.; Choi, K.-S. Effect of a Cobalt-Based Oxygen Evolution Catalyst on the Stability and the Selectivity of Photo-Oxidation Reactions of a WO_3 Photoanode. *Chem. Mater.* **2011**, *23*, 1105–1112. [CrossRef]
18. Phuan, Y.W.; Ong, W.-J.; Chong, M.N.; Ocon, J.D. Prospects of electrochemically synthesized hematite photoanodes for photoelectrochemical water splitting: A review. *J. Photochem. Photobiol. C* **2017**, *33*, 54–82. [CrossRef]
19. Wu, Y.-C.; Song, R.-J.; Li, J.-H. Recent advances in photoelectrochemical cells (PECs) for organic synthesis. *Org. Chem. Front.* **2020**, *7*, 1895–1902. [CrossRef]
20. Labinger, J.A.; Bercaw, J.E. Understanding and exploiting C–H bond activation. *Nature* **2002**, *417*, 507–514. [CrossRef] [PubMed]
21. Rocha, R.S.; Reis, R.M.; Lanza, M.R.; Bertazzoli, R. Electrosynthesis of methanol from methane: The role of V_2O_5 in the reaction selectivity for methanol of a $TiO_2/RuO_2/V_2O_5$ gas diffusion electrode. *Electrochim. Acta* **2013**, *87*, 606–610. [CrossRef]
22. Boyd, M.J.; Latimer, A.A.; Dickens, C.F.; Nielander, A.C.; Hahn, C.; Nørskov, J.K.; Higgins, D.C.; Jaramillo, T.F. Electro-Oxidation of Methane on Platinum under Ambient Conditions. *ACS Catal.* **2019**, *9*, 7578–7587. [CrossRef]
23. Arnarson, L.; Schmidt, P.S.; Pandey, M.; Bagger, A.; Thygesen, K.S.; Stephens, I.E.L.; Rossmeisl, J. Fundamental limitation of electrocatalytic methane conversion to methanol. *Phys. Chem. Chem. Phys.* **2018**, *20*, 11152–11159. [CrossRef] [PubMed]
24. Luo, J.-H.; Hong, Z.-S.; Chao, T.-H.; Cheng, M.-J. Quantum Mechanical Screening of Metal-N_4-Functionalized Graphenes for Electrochemical Anodic Oxidation of Light Alkanes to Oxygenates. *J. Phys. Chem. C* **2019**, *123*, 19033–19044. [CrossRef]
25. Fornaciari, J.C.; Primc, D.; Kawashima, K.; Wygant, B.R.; Verma, S.; Spanu, L.; Mullins, C.B.; Bell, A.T.; Weber, A.Z. A Perspective on the Electrochemical Oxidation of Methane to Methanol in Membrane Electrode Assemblies. *ACS Energy Lett.* **2020**, *5*, 2954–2963. [CrossRef]
26. Lee, B.; Hibino, T. Efficient and selective formation of methanol from methane in a fuel cell-type reactor. *J. Catal.* **2011**, *279*, 233–240. [CrossRef]
27. Heo, P.; Ito, K.; Tomita, A.; Hibino, T. A Proton-Conducting Fuel Cell Operating with Hydrocarbon Fuels. *Angew. Chem. Int. Ed.* **2008**, *47*, 7841–7844. [CrossRef]
28. Yamanaka, I.; Hasegawa, S.; Otsuka, K. Partial oxidation of light alkanes by reductive activated oxygen over the (Pd-black + $VO(acac)_2$/VGCF) cathode of H_2–O_2 cell system at 298 K. *Appl. Catal. A* **2002**, *226*, 305–315. [CrossRef]
29. Kim, R.S.; Surendranath, Y. Electrochemical Reoxidation Enables Continuous Methane-to-Methanol Catalysis with Aqueous Pt Salts. *ACS Cent. Sci.* **2019**, *5*, 1179–1186. [CrossRef]
30. O'Reilly, M.E.; Kim, R.S.; Oh, S.; Surendranath, Y. Catalytic Methane Monofunctionalization by an Electrogenerated High-Valent Pd Intermediate. *ACS Cent. Sci.* **2017**, *3*, 1174–1179. [CrossRef]
31. Cha, H.G.; Choi, K.-S. Combined biomass valorization and hydrogen production in a photoelectrochemical cell. *Nat. Chem.* **2015**, *7*, 328–333. [CrossRef]
32. Song, H.; Meng, X.; Wang, Z.-j.; Liu, H.; Ye, J. Solar-Energy-Mediated Methane Conversion. *Joule* **2019**, *3*, 1606–1636. [CrossRef]
33. Lee, J.; Yang, J.; Moon, J.H. Solar Cell-Powered Electrochemical Methane-to-Methanol Conversion with CuO/CeO_2 Catalysts. *ACS Energy Lett.* **2021**, *6*, 893–899. [CrossRef]
34. Fuku, K.; Sayama, K. Efficient oxidative hydrogen peroxide production and accumulation in photoelectrochemical water splitting using a tungsten trioxide/bismuth vanadate photoanode. *Chem. Commun.* **2016**, *52*, 5406–5409. [CrossRef] [PubMed]
35. Fuku, K.; Miyase, Y.; Miseki, Y.; Gunji, T.; Sayama, K. Enhanced Oxidative Hydrogen Peroxide Production on Conducting Glass Anodes Modified with Metal Oxides. *ChemistrySelect* **2016**, *1*, 5721–5726. [CrossRef]
36. Murcia-López, S.; Villa, K.; Andreu, T.; Morante, J.R. Improved selectivity for partial oxidation of methane to methanol in the presence of nitrite ions and BiVO4 photocatalyst. *Chem. Commun.* **2015**, *51*, 7249–7252. [CrossRef]
37. Cheng, J.; Li, Z.; Haught, M.; Tang, Y. Direct methane conversion to methanol by ionic liquid-dissolved platinum catalysts. *Chem. Commun.* **2006**, 4617–4619. [CrossRef]
38. Tomita, A.; Nakajima, J.; Hibino, T. Direct Oxidation of Methane to Methanol at Low Temperature and Pressure in an Electrochemical Fuel Cell. *Angew. Chem. Int. Ed.* **2008**, *47*, 1462–1464. [CrossRef]
39. Santos, M.C.L.; Nunes, L.C.; Silva, L.M.G.; Ramos, A.S.; Fonseca, F.C.; de Souza, R.F.B.; Neto, A.O. Direct Alkaline Anion Exchange Membrane Fuel Cell to Converting Methane into Methanol. *ChemistrySelect* **2019**, *4*, 11430–11434. [CrossRef]
40. Amenomiya, Y.; Birss, V.I.; Goledzinowski, M.; Galuszka, J.; Sanger, A.R. Conversion of Methane by Oxidative Coupling. *Catal. Rev.* **1990**, *32*, 163–227. [CrossRef]
41. Spinner, N.; Mustain, W.E. Electrochemical Methane Activation and Conversion to Oxygenates at Room Temperature. *ECS Trans.* **2013**, *53*, 1–20. [CrossRef]

42. Ma, M.; Jin, B.J.; Li, P.; Jung, M.S.; Kim, J.I.; Cho, Y.; Kim, S.; Moon, J.H.; Park, J.H. Ultrahigh electrocatalytic conversion of methane at room temperature. *Adv. Sci.* **2017**, *4*, 1700379. [CrossRef]
43. Ma, M.; Oh, C.; Kim, J.; Moon, J.H.; Park, J.H. Electrochemical CH_4 oxidation into acids and ketones on ZrO_2:$NiCo_2O_4$ quasi-solid solution nanowire catalyst. *Appl. Catal. B* **2019**, *259*, 118095. [CrossRef]
44. Lu, J.; Zhu, C.; Pan, C.; Lin, W.; Lemmon John, P.; Chen, F.; Li, C.; Xie, K. Highly efficient electrochemical reforming of CH_4/CO_2 in a solid oxide electrolyser. *Sci. Adv.* **2018**, *4*, eaar5100. [CrossRef] [PubMed]
45. Zhu, C.; Hou, S.; Hu, X.; Lu, J.; Chen, F.; Xie, K. Electrochemical conversion of methane to ethylene in a solid oxide electrolyzer. *Nat. Commun.* **2019**, *10*, 1173. [CrossRef] [PubMed]
46. Sinev, M.Y.; Tulenin, Y.P.; Kalashnikova, O.V.; Bychkov, V.Y.; Korchak, V.N. Oxidation of methane in a wide range of pressures and effect of inert gases. *Catal. Today* **1996**, *32*, 157–162. [CrossRef]
47. Yamamoto, S.; Alcauskas, J.B.; Crozier, T.E. Solubility of methane in distilled water and seawater. *J. Chem. Eng. Data* **1976**, *21*, 78–80. [CrossRef]
48. Wei, J.; Yang, J.; Wen, Z.; Dai, J.; Li, Y.; Yao, B. Efficient photocatalytic oxidation of methane over β-Ga_2O_3/activated carbon composites. *RSC Adv.* **2017**, *7*, 37508–37521. [CrossRef]
49. Gao, J.; Xu, C.-Q.; Hung, S.-F.; Liu, W.; Cai, W.; Zeng, Z.; Jia, C.; Chen, H.M.; Xiao, H.; Li, J.; et al. Breaking Long-Range Order in Iridium Oxide by Alkali Ion for Efficient Water Oxidation. *J. Am. Chem. Soc.* **2019**, *141*, 3014–3023. [CrossRef]
50. Liang, Z.; Li, T.; Kim, M.; Asthagiri, A.; Weaver Jason, F. Low-temperature activation of methane on the IrO(110) surface. *Science* **2017**, *356*, 299–303. [CrossRef]